

Chasing Consistency in Text-to-3D Generation from a Single Image

Yichen Ouyang¹ Wenhao Chai² Jiayi Ye¹
Dapeng Tao⁴ Yibing Zhan^{3*} Gaoang Wang^{1*}

¹Zhejiang University ²University of Washington ³JD Explore Academy ⁴Yunnan University

Abstract

Text-to-3D generation from a single-view image is a popular but challenging task in 3D vision. Although numerous methods have been proposed, existing works still suffer from the inconsistency issues, including 1) semantic inconsistency, 2) geometric inconsistency, and 3) saturation inconsistency, resulting in distorted, overfitted, and over-saturated generations. In light of the above issues, we present **Consist3D**, a three-stage framework Chasing for semantic-, geometric-, and saturation-**Consistent** Text-to-**3D** generation from a single image, in which the first two stages aim to learn parameterized consistency tokens, and the last stage is for optimization. Specifically, the semantic encoding stage learns a token independent of views and estimations, promoting semantic consistency and robustness. Meanwhile, the geometric encoding stage learns another token with comprehensive geometry and reconstruction constraints under novel-view estimations, reducing overfitting and encouraging geometric consistency. Finally, the optimization stage benefits from the semantic and geometric tokens, allowing a low classifier-free guidance scale and therefore preventing over-saturation. Experimental results demonstrate that Consist3D produces more consistent, faithful, and photo-realistic 3D assets compared to previous state-of-the-art methods. Furthermore, Consist3D also allows background and object editing through text prompts.

1 Introduction

Recently, text-to-3D generation from a single image has emerged as an active research area, with the goal of personalizing 3D assets using a reference image. This field has been explored extensively in previous literature (Raj et al. 2023; Seo et al. 2023), often relying on shape estimation or few-shot finetuning as the prior and score distillation sampling (Poole et al. 2022) as the optimizer. Even though numerous methods have been proposed, they still suffer from inconsistency issues. For instance, 1) misguided semantics caused by inaccurate shape estimations. 2) distorted geometric caused by overfitting on the reference view. 3) over-saturated color caused by score distillation sampling.

Shape estimation methods (Nichol et al. 2022; Jun and Nichol 2023; Yu et al. 2023; Sanghi et al. 2023), including point cloud estimation, sketch estimation, etc., aim to aid

*Corresponding authors.

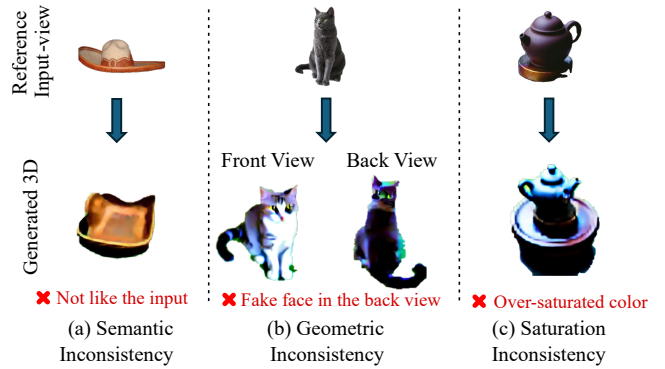
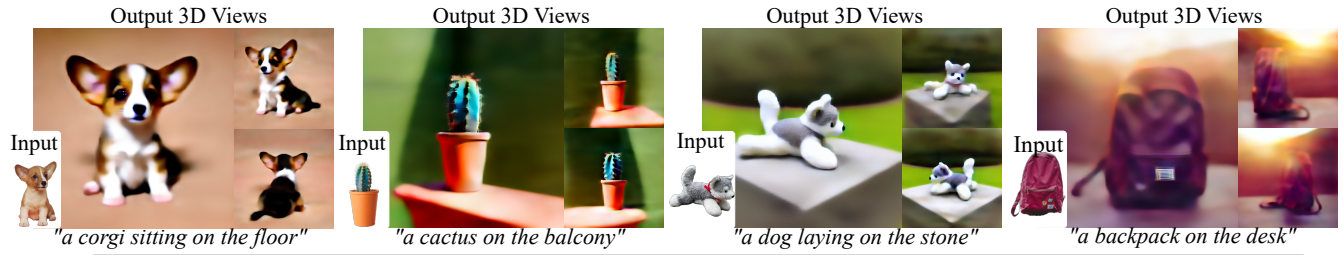


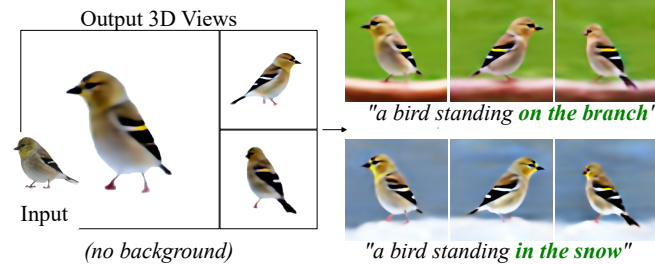
Figure 1: **Inconsistency issues.** (a) The semantic inconsistency: the generated object looks like a box instead of hat. (b) The geometric consistency: the generated cat’s face exists in the back view of a cat whose face originally towards the front view. (c) The saturation inconsistency: the rendering of the generated teapot is oversaturated compared with the original teapots color.

text-to-3D generation by providing an estimated 3D prior for each novel view. However, they often inaccurately estimate the 3D priors, which results in misguided semantics, especially when a single-view image is the only input, because, in such a situation, there is no enough information provided for estimating 3D priors. Few-shot fine-tuning methods (Ruiz et al. 2022; Zhang et al. 2023) aim at personalizing a text-to-image generative model with several images with a common subject. However, when only one single input image is provided for training, they often lead to geometric inconsistency across novel views because of overfitting on the reference single view. The score distillation sampling method (Poole et al. 2022) aims to lift the 2D generations to 3D assets. This lifting process needs to ensure that the generation under each viewing angle is stable enough, so the fidelity of saturation is sacrificed for stability with a high classifier-free guidance scale applied. Therefore, current methods for generating 3D assets from a single image face challenges with inconsistency in semantics, geometry, and saturation, often resulting in distorted and over-saturated generations, as illustrated in Fig. 1. Enhancing semantic and

(a) Single-view Text-to-3D Generation



(b) Background Editing



(c) Object Editing

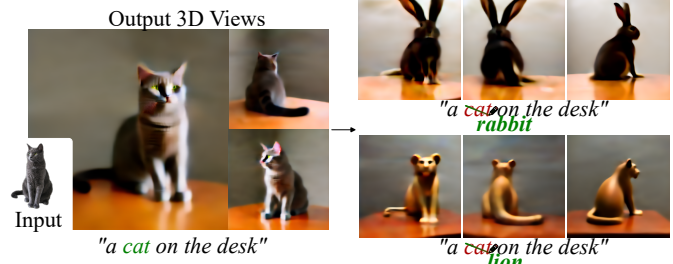


Figure 2: **Effectiveness of our method.** (a) Single-view Text-to-3D generation: each case with one single input image and 3 novel views rendered from the 3D generations. (b) Background Editing: the background of the generation can be edited by prompt, and the option for no background is provided as well. (c) Object Editing: the object of the generation can be edited by prompt. For example, we can change the “cat” into “rabbit” or “lion” without changing the input image.

geometric consistency across seen and unseen views while being robust to inaccurate shape estimations, and mitigating color distortion in optimization, is imperative for achieving satisfactory 3D generation results.

In this paper, we present **Consist3D**, a semantic-geometric-saturation **Consistent** approach for photo-realistic and faithful text-to-**3D** generation from a single image. We address the three inconsistency issues (as shown in Fig. 1) by introducing a three-stage framework, including a semantic encoding stage, a geometric encoding stage, and an optimization stage. In the first stage, a parameterized identity token is trained independently of shape priors, enhancing robustness to misguidance and relieving the semantic-inconsistency problem. In the second stage, a geometric token is trained with comprehensive geometry and reconstruction constraints, overcoming single-view overfitting issues and further enhancing geometric consistency between different views. In the third stage, the optimization process benefits from the semantic token and geometric token, allowing low classifier-free guidance (CFG) scales, therefore addressing the saturation-inconsistency issue and enabling background and object editing through text prompt.

The experiments highlight the strengths of Consist3D in generating high-fidelity 3D assets with robust consistency, while remaining faithful to the input single image and text prompts. As shown in Fig. 2 (a), compared to baseline methods, our generated results exhibit improved consistency and more reasonable saturation. Notably, our approach enables background editing (Fig. 2 (b)) and object editing (Fig. 2 (c)) through text prompt, without changing the input image. We summarize our contribution as follows:

- To our knowledge, we are the first to explore the semantic-geometric-saturation consistency problems in text-to-3D generation, and accordingly, we propose **Consist3D**, an approach for consistent text-to-3D generation, background and object editing from a single image.
- Our Consist3D consists of a three-stage framework, including a semantic encoding stage, a geometric encoding stage, and an optimization stage, and can generate robust, non-overfitted, natural-saturated 3D results under a low classifier-free guidance scale.
- Extensive experiments are conducted. Compared with prior arts, the experimental results demonstrate that Consist3D produces faithful and photo-realistic 3D assets with significantly better consistency and fidelity.

2 Related Works

2.1 Personalized Text-to-Image Generation

Text-to-image (T2I) generative models (Rombach et al. 2022; Podell et al. 2023; Saharia et al. 2022; Ramesh et al. 2022; Xue et al. 2023) have significantly expanded the ways we can create 2D images with text prompt in multi-modality field (Chai and Wang 2022). With text-to-image (T2I) synthesis enhanced by controllable denoising diffusion models (Cao et al. 2023; Huang et al. 2023a; Kwarar et al. 2023; Huang et al. 2023b), personalizing text-to-image generation has become the emerging focus of research, which aims to generate images faithful to a specific subject. This area has seen considerable exploration (Dhariwal and Nichol 2021; Ho and Salimans 2022; Zhang and Agrawala 2023; Gal et al. 2022; Ruiz et al. 2022; Wu et al. 2023). For example, textual inversion methods (Yang et al. 2023; Zhang et al. 2023;

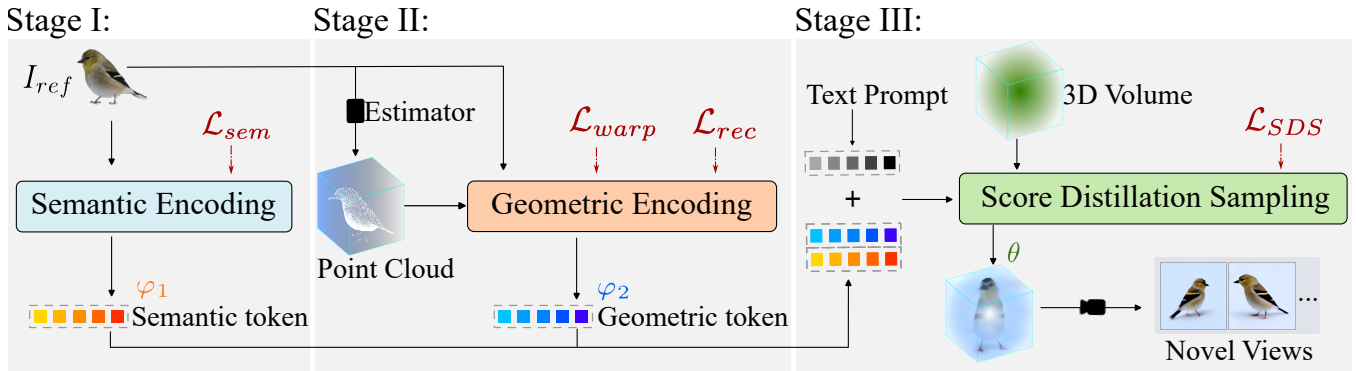


Figure 3: **Pipeline.** Stage I. A single-view image is input to the semantic encoding module, and a semantic token is trained with sem loss. Stage II. The single-view image is the input and used to estimate a point cloud as the shape guidance to apply condition on the geometric encoding module, and a geometric token is trained with warp loss and rec loss. Stage III. A randomly initialized 3D volume is the input and the two tokens trained previously is utilized together with tokenized text prompt as the condition, and this 3D volume is trained into a 3D model faithful to the reference single image.

Huang et al. 2023c; Voynov et al. 2023) learn parameterized textual descriptions from a set of images sharing a common subject. This extends the T2I tasks to image-to-image generation, essentially realizing subject-driven personalization. To enhance textual inversions efficiently, there currently emerges a lot of few-shot finetuning approaches. Typically, DreamBooth (Ruiz et al. 2022) learns parameterized adapters (*i.e.*, LoRA (Hu et al. 2021)) for the generative network, instead of parameterizing the textual descriptions. In another direction, ControlNet (Zhang and Agrawala 2023), Composer (Huang et al. 2023a), and T2I-Adapter (Mou et al. 2023) offer guidance to diffusion models, facilitating custom-defined constraints over the generation process, and yielding controllable personalization.

2.2 Personalized Text-to-3D Generation

Personalized text-to-3D generation has gained interest by extending successful personalized T2I models, aiming at generating 3D assets from a few images (Raj et al. 2023; Xu et al. 2023). Most current approaches (Metzer et al. 2022; Raj et al. 2023) apply few-shot tuning (e.g., DreamBooth) for personalization and score distillation sampling (SDS) (Poole et al. 2022) for optimization. A generalized DreamFusion approach combines few-shot tuning on a few images for personalization and estimations from Zero-1-to-3 (Liu et al. 2023) as the shape priors, followed by SDS optimization. However, shape priors estimated by Zero-1-to-3 are often view-inconsistent, resulting in low-quality generations. Another work, DreamBooth3D (Raj et al. 2023) enables personalized 3D generation from 3-5 images via joint few-shot tuning and SDS optimization. However, when the input views are decreased to 1, overfitting on limited views leads to reconstruction failures and geometric inconsistency for novel views. Generating personalized 3D assets from only one single input image remains challenging (Cai et al. 2023; Gu et al. 2023a; Deng et al. 2023; Gu et al. 2023b; Xing et al. 2022; Lin et al. 2022). 3DFuse enables one-shot tuning on a single image and an estimated point cloud as guidance for a ControlNet for personalization, which per-

forms together with SDS optimization. However, semantic and geometric inconsistency across views persists, as the point cloud estimation lacks accuracy, and one-shot tuning overfits the given view. This results in blurred, low-fidelity outputs. Score distillation sampling (SDS) optimizes 3D volume representations using pretrained text-to-image models, first introduced in DreamFusion (Poole et al. 2022). With the introduction of SDS, high-quality text-to-3D generation has been achieved in many previous works (Lin et al. 2023; Tang et al. 2023; Tsalicoglou et al. 2023; Chen et al. 2023; Wang et al. 2023). The insight of SDS is that under high classifier-guidance (CFG) scale, the generation of T2I model is stable enough under each text prompt, therefore enabling the 3D volume to converge. However, current works find that high CFG scale harms quality of the generations, leading to over-saturated results (Wang et al. 2023).

3 Method

3.1 Overview

The input to our approach is a single image I_{ref} and a text prompt y . We aim to generate a θ parameterized 3D asset that captures the subject of the given image while being faithful to the text prompt. To achieve consistent 3D generation in the encoding process, we learn semantic consistency token and geometric consistency token, parameterized by φ_1 and φ_2 , respectively. Overall, the parameters we need to optimize are $\varphi_1, \varphi_2, \theta$, and the optimization goal can be formulated as follows,

$$\min_{\varphi_1, \varphi_2, \theta} \mathcal{L}(g(\theta, c), \epsilon(I_{ref}, y, y_{\varphi_1, \varphi_2}, c)), \quad (1)$$

where \mathcal{L} is the loss function, c is the camera view, g is a differential renderer, and ϵ is the diffusion model used to generate image using both text prompt y and learned prompt y_{φ_1, φ_2} under the given view.

To facilitate the optimization of the parameters $\varphi_1, \varphi_2, \theta$, we adopt two encoding stages and one score distillation sampling stage in our pipeline (Fig. 3). In the first stage, we propose semantic encoding and fine-tune a pretrained diffusion

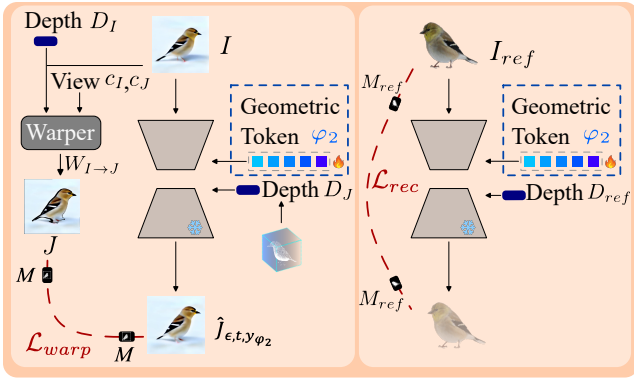


Figure 4: **Geometric encoding.** We adopt ControlNet with depth guidance for the generation. The training object is \mathcal{L}_{warp} and \mathcal{L}_{rec} . The \mathcal{L}_{warp} calculated loss between two neighboring views with warp mask under novel views, and the \mathcal{L}_{rec} calculated loss between the single input image and the generation with reference mask under reference view.

model $\epsilon_{pretrain}$ to learn a semantic token parameterized by φ_1 , aiming at encapsulating the subject of the given image. In the second encoding stage, we propose geometric encoding to learn a geometric token parameterized by φ_2 , with carefully designed geometry constraints and reconstruction constraints. In the score distillation sampling stage, we propose a low-scale optimization for θ parameterized 3D volume presentations, benefited specifically from the enhanced consistency with the proposed tokens.

3.2 Semantic Encoding

The semantic encoding stage aims to learn the semantic token parameterized by φ_1 . The semantic token can be further incorporated with the text prompt to faithfully reconstruct the reference view image I_{ref} with consistent semantics. Specifically, we use the single image I_{ref} as the input to do one-shot fine-tuning to obtain the semantic token parameterized by φ_1 to represent the given image as follows,

$$\min_{\varphi_1} \mathcal{L}_{sem}(\varphi_1) := \mathbb{E}_{x, \epsilon, t} [w(t) \cdot \|\epsilon_{pretrain}(I_{ref}, t, y_{\varphi_1}) - \epsilon_t\|_2^2], \quad (2)$$

where y_{φ_1} is a prompt containing the semantic token, $\epsilon_{pretrain}$ represents the pretrained stable diffusion model, ϵ_t is the noise scheduled at time step t , and $w(t)$ is the scaling factor which will be discussed in detail in Section 3.4.

We use the same training setting to DreamBooth (Ruiz et al. 2022), which enables few-shot personalization of text-to-image models using multiple reference images of a subject. Specifically, we adopt DreamBooth for one-shot personalization, which optimizes φ_1 by Eq. 2 to identify the single-view image. Notably, with only one image I_{ref} as the input, naive DreamBooth tends to overfit not only the subject but also the view of the reference image, leading to inconsistent generations under novel views. To address this, we propose the second encoding stage to improve the geometric consistency.

3.3 Geometric Encoding

In the second stage, we propose geometric encoding (Fig. 4), which aims to solve the overfitting and inconsistency issues by encapsulating warp and reconstruction consistency into what we term geometric token, parameterized by φ_2 .

To achieve warp and semantic consistency, the overall objective $\mathcal{L}_{geometric}$ combines the two terms \mathcal{L}_{warp} and \mathcal{L}_{rec} (Eq. 3). Notably, the consistency token from this encoding stage does not contain standalone semantics. Due to depth guidance, its semantic is conditioned on view c , encapsulating inherent 3D consistency of generation. By incorporating this token into prompts, we enhance geometric consistency of diffusion model outputs across different views.

$$\mathcal{L}_{geometric}(\varphi_2 | c_I) = \mathcal{L}_{warp}(\varphi_2 | c_I) + \mathcal{L}_{rec}(\varphi_2 | c_{ref}), \quad (3)$$

where c_I defines the sampled camera view for image I , c_{ref} is the given input reference view. The warp loss and the reconstruction loss are demonstrated as follows.

Warp Loss The warp loss aims to ensure a consistent transition between two camera views, c_I and c_J , with a learnable geometric token parameterized by φ_2 . The loss is formulated as follows,

$$\min_{\varphi_2} \mathcal{L}_{warp}(\varphi_2 | c_I) := \mathbb{E}_{x, \epsilon, t, c_I} [w(t) \cdot \|(\hat{J}_{\epsilon, t, y, \varphi_2} - \mathcal{W}_{I \rightarrow J}(I, D)) \cdot M\|_2^2], \quad (4)$$

where $\hat{J}_{\epsilon, t, y, \varphi_2}$ is the generated image from the diffusion model under the view c_J guided by the learnable geometric token φ_2 , $\mathcal{W}_{I \rightarrow J}(I, D)$ is the warp operator that transfers the image I from the view c_I to the view c_J based on the depth map D , and M is the warp mask indicating the visible points in both views. Note that the warper $\mathcal{W}_{I \rightarrow J}$ is a deterministic function when the two views and the depth map are known.

The novel view image $\hat{J}_{\epsilon, t, y, \varphi_2}$ is generated from the input view c_I based on the pretrained diffusion model $\epsilon_{pretrain}$ as follows,

$$\hat{J}_{\epsilon, t, y, \varphi_2} = \alpha_t I + \sigma_t \epsilon_{pretrain}(I, t, y_{\varphi_2}, D_J), \quad (5)$$

where α_t and σ_t are predefined parameters in the pretrained diffusion model $\epsilon_{pretrain}$ conditioned on time step t , D_J is the estimated depth map under view c_J . Here, ControlNet (Zhang and Agrawala 2023) is adopted as the pretrained diffusion model with depth map as conditions. With the warp loss, the geometric token enables the diffusion model to have the capability of cross-view generation with the learnable parameter φ_2 .

In the implementation, we use Point-E (Nichol et al. 2022) to generate the 3D point cloud and then obtain the depth map of the input image. Initially, we use the input reference view c_{ref} as c_I , and then sample a neighboring view as c_J with a small view change. After multiple steps, views from 360 degrees will be sampled.

Reconstruction Loss The reconstruction loss ensure the geometric token φ_2 to retain subject semantics under the ref-

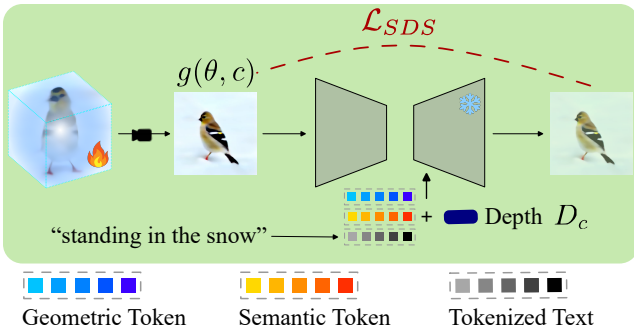


Figure 5: **Score distillation sampling.** A rendered image of a 3D volume is utilized as the input and a depth ControlNet with low CFG scales is utilized for generation. For the text condition, we combine the semantic token and geometric token with tokenized texts, which enables background editing and object editing through prompt.

erence view c_{ref} with the reference image I_{ref} as follows,

$$\min_{\varphi_2} \mathcal{L}_{rec}(\varphi_2 | c_{ref}) := \mathbb{E}_{x, \epsilon, t} [w(t) \cdot \|\epsilon_{pretrain}(I_{ref} \cdot M_{ref}, t, y_{\varphi_2}, D_{ref}) - \epsilon_t \cdot M_{ref}\|_2^2], \quad (6)$$

where D_{ref} is the depth map image and M_{ref} is the object mask. This enforces the model to generate the ground truth image when guided by the true depth, ensuring consistent subject identity.

3.4 Low-scale Score Distillation Sampling

In the score distillation sampling stage (Fig. 5), we use prompts y_{φ_1, φ_2} with both φ_1 parameterized semantic token and φ_2 parameterized geometric token, guided by the depth map D_c under the sampled view c . The aim of this stage is to learn a 3D volume parameterized by θ . Specifically, we adopt the deformed SDS formulation as follows:

$$\nabla_{\theta} \mathcal{L}_{SDS}(\theta) := \mathbb{E}_{t, \epsilon, c} [w(t) \cdot (\epsilon_{pretrain}(x_t, t, y_{\varphi_1, \varphi_2}, D_c) - \epsilon_t) \frac{\partial g(\theta, c)}{\partial \theta}], \quad (7)$$

where the time step $t \sim \mathcal{U}(0.02, 0.98)$, noise $\epsilon_t \sim \mathcal{N}(0, \mathcal{I})$, and $g(\theta, c)$ is the rendered image from the 3D volumes parameterized by θ under camera view c , $x_t = \alpha_t g(\theta, c) + \sigma_t \epsilon$.

The scaling factor $w(t)$ in Eq. 7 allows flexibly tuning the degree of conditionality in classifier-free guidance (CFG) for text-to-image generation (Ho and Salimans 2022). Higher scales impose stronger conditional constraints, while lower scales enable more unconditional generation. In 2D text-to-image, the CFG scale is typically set between 7.5 and 10 to balance quality and diversity.

Typically, high CFG scales (up to 100) are required for text-to-3D optimization as DreamFusion proposed. However, excessively high scales can impair image quality and diversity (Wang et al. 2023). Our consistency tokens learned in the first two stages enhance semantic and geometric consistency, allowing high-quality distillation even at low scales (< 25). This achieves photo-realistic, natural-saturated 3D generations faithfully adhering to the subject.

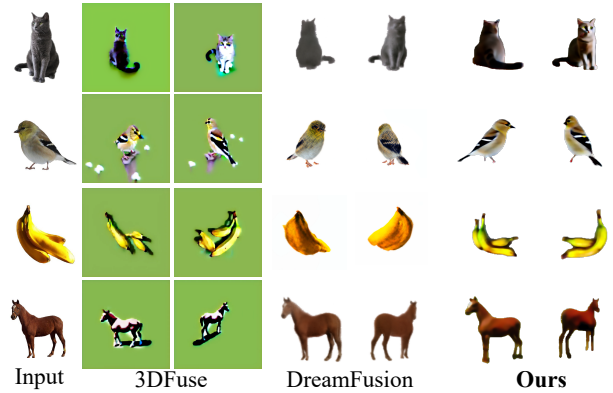


Figure 6: **Comparison with baselines (text-to-3D generation from a single image).** The first column is the single input image. The following columns are results of 3DFuse, DreamFusion and Consist3D(Ours), separately. DreamFusion cannot correctly synthesize photo-realistic images and thin objects. 3DFuse is strongly troubled by inconsistency issues. However, the generation results of our method are not only faithful to the reference but also natural saturated, with good consistencies.

4 Experiments

4.1 Implementation Details

We use Stable Diffusion (Rombach et al. 2022) as the generative model with CLIP (Radford et al. 2021) text encoder and LoRA (Hu et al. 2021) as the adapter technique for fine-tuning. As for the representation of the 3D field, we adopt Score Jacobian Chaining (SJC) (Wang et al. 2022). Encoding takes half an hour for each of the two stages, and distillation takes another hour. Specifically, Stage I semantic encoding uses $1k$ optimization steps with LoRA. Stage II geometric encoding uses $2k$ optimization steps with LoRA. Stage III uses $10k$ optimization steps for SJC.

4.2 Datasets

We evaluate Consist3D on a wide range of image collections, where the categories include animals, toys, and cartoon characters, and each subject is presented with a single-view capture. The sources of the image collections includes in-the-wild images selected from ImageNet, cartoon characters collected from the Internet, and images from the DreamBooth3D dataset. We optimize each 3D asset corresponding to the given single-view image with several different prompts and backgrounds, demonstrating faithful and photo-realistic 3D generation results in diversity.

4.3 Performance Comparison

Text-to-3D Generation from a Single Image We compare our results with two baselines (e.g., DreamFusion (Poole et al. 2022) and 3DFuse (Seo et al. 2023)) in single-image based text-to-3D generation task, because they are the most related to our method and are representative works in the field of personalized 3D generation. Notably, the original implementation of DreamFusion is a text-

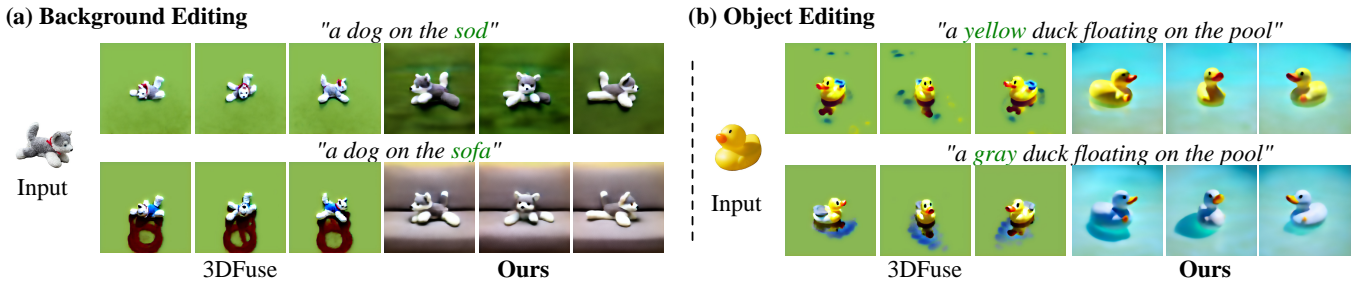


Figure 7: **Comparison with baselines (background and object editing)**. (a) 3DFuse cannot correctly generate the background of the dog, while our method generates “sod” and “sofa” properly. (b) With the object “yellow duck” changed to “gray duck”, 3DFuse only generates a duck with small gray wings, while our method changes the whole body to gray successfully.

Methods	anya	banana	bird	butterfly	cat	clock	duck	hat	horse	shark	sneaker	sunglasses	Average
DreamFusion	80.71	69.80	71.93	65.76	72.76	69.38	80.34	71.10	75.40	67.31	63.46	60.59	70.71
3DFuse	70.31	71.72	73.41	75.12	67.19	64.60	78.84	62.63	68.52	71.81	67.33	74.05	70.46
Consist3D (ours)	80.05	77.22	80.99	82.00	72.85	71.47	84.13	87.34	77.96	72.04	73.59	77.04	78.06

Table 1: **CLIP score**. The bold ones in the figure are the highest CLIP Scores in each category. The performance of our method surpasses baselines comprehensively.

Method	saturation	geometric	semantic	fidelity	clarity	Average
DreamFusion	65.40	72.20	76.07	79.29	76.10	73.81
3DFuse	69.87	73.51	63.58	72.51	77.54	71.40
Consist3D (ours)	89.73	77.29	85.35	82.20	79.36	82.79

Table 2: **User study**. The bold ones in the figure are the best scores in each type of problem. Our method surpasses baselines in both consistency and quality.

to-3D structure. Therefore, we initially utilized a single-view image along with DreamBooth for one-shot tuning, and then incorporated the shape prior estimated by Zero-1-to-3 for DreamFusion to produce 3D assets, following the implementation of the official open source code. Our results are bench-marked against the baseline DreamFusion and 3DFuse, as Fig. 6 shows. In the case of 3DFuse, we adhere to the original configuration established by its authors. We notice that DreamFusion suffers from incorrect shape prior estimations and gives unnatural results (Fig. 6), due to the super-high guidance scale. The generation quality of 3DFuse is strictly limited by the estimated point cloud prior, and even a slightly incorrect depth map can lead to completely wrong generations. Furthermore, its generated objects are not faithful enough to the given reference view, most time with blurred edges and overfitting problems. In contrast, our work can generate objects that are faithful to the input image, and achieve a more natural and photo-realistic reconstruction, not leaning towards the artistic model.

Background and Object Editing For background editing, we compare our results with 3DFuse, since DreamFusion does not provide an option to edit the background. As Fig. 7 (a) shows, 3DFuse is unable to correctly generate the correct background, even if we have turned on the background generation option on. In contrast, our model is capa-

ble of editing the background for the reconstructed object by diverse prompts. For object editing, we compare our results with 3DFuse as well. As Fig. 7 (b) shows, 3DFuse is also unable to correctly change the object with the unchanged input image while our model can make it.

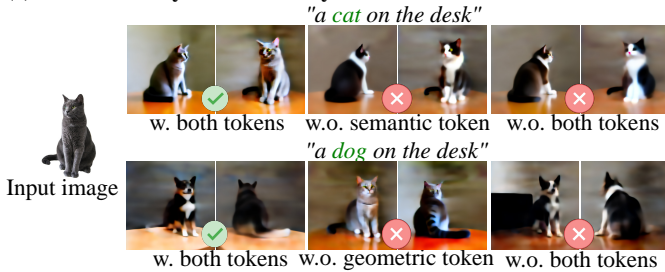
4.4 Quantitative Evaluation

We compare our method with two baselines under 12 categories as shown in Tab. 1. The data for these 12 categories include unseen-domain anime from Internet, in-the-wild images from ImageNet, and synthetic datasets from the DreamBooth Dataset. CLIP Score (Hessel et al. 2022) is a measure of image-text similarity. The higher the value, the more semantically the image and text match. We extend it to image-to-image similarity, which measures the similarity between the generated result and a given single-view image. To extend and calculate CLIP Score, we first re-describe the reference image with BLIP-2, and for fairness, remove the background description. Then for the reconstruction results of the 3D generation methods, we sample 100 camera positions, and for each position’s sampled image, calculate the CLIP Score with the previously obtained description, and take the average separately for each method. Our method far surpasses the baselines in most categories, which means our generations are more faithful to the reference subject.

4.5 User Study

We have conducted a user study with 137 participants, which is shown in Table. 2. We have asked the participants to choose their preferred result in terms of saturation consistency, geometric consistency, semantic consistency, overall fidelity, and overall clarity among DreamFusion, 3DFuse, and Consist3D (Ours). The results show that Consist3D generates 3D scenes that the majority of people judge as having better consistency and overall quality than other methods.

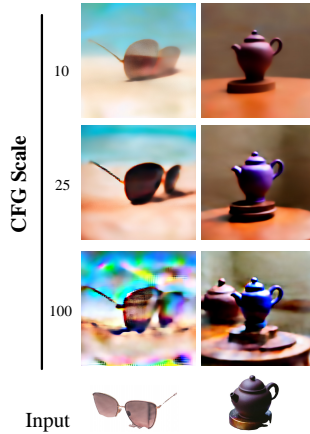
(a) Ablation study on consistency tokens



(b) Ablation study on warp loss and rec loss



(c) Ablation Study on CFG Scales



(d) Ablation Study on Seed Values

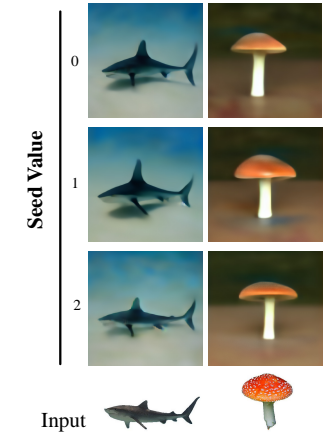


Figure 8: **Ablation study.** (a) Consistency Tokens. The first row: without semantic token, the generation is not faithful to the input image. The second row: without geometric token, the generation is not consistent in novel views and fails to do object editing. (b) Losses. Without \mathcal{L}_{rec} or \mathcal{L}_{warp} , the generation becomes not faithful to the input image or fails to generate correct background. (c) CFG Scales. The 3D synthesis of sunglasses and teapot under CFG scales of 10, 25, 100, separately. Results at lower scale are more natural saturated, while the generations at higher scale tend to be with over-saturated color. (d) Seed Values. The 3D synthesis of shark and mushroom under seed values of 0, 1, 2 demonstrates our method is robust to different seeds, with the generations slightly changed.

4.6 Ablation Studies

Consistency Tokens In Fig. 8 (a), we show ablation studies for the two consistency tokens. First, we test the role of semantic token on single-image text-to-3D generation, and we find that removing the semantic token will cause the generated object’s semantics to be inconsistent with the input image. In addition, we test the role of geometric token on object editing. We find that removing the geometric token leads to inconsistent generations under novel views, and the generated object could not be edited, which indirectly proves that the geometric token emphasizes the shape’s geometric consistency across different viewing angles, while not over-fitting to the view of the input image.

Losses In Fig. 8 (b), we test the roles of warp loss \mathcal{L}_{warp} and reconstruction loss \mathcal{L}_{rec} in the geometric encoding stage. With only the loss \mathcal{L}_{rec} applied, the model cannot generate correct background but the object is faithful to the input image. With only the loss \mathcal{L}_{warp} applied, the model generates geometric consistent 3D asset, but the background is not faithful to the input text. With both \mathcal{L}_{warp} and \mathcal{L}_{rec} applied, the results are faithful to the input image and text prompt while keeping geometric consistency with object and background correctly generated.

CFG Scales In the ablation study for score distillation sampling (Fig. 8 (c)), we vary the CFG scale to 10, 25, and 100, showing our low-scale distillation improves 3D quality. The consistency tokens reduce scale requirements for photo-realistic 3D generation. Our method achieves good, diverse results with low scales (below 25).

Seed Values We experiment with fixed prompts and changing random seeds to verify the robustness of our ap-

proach as Fig. 8 (d) shows. The results demonstrate that our approach is not sensitive to random seeds.

5 Limitation and Future Work

Our method fails when the point cloud estimation is severely distorted. Moreover, if overly complex background prompts are used, the model may not be able to generate high-detail backgrounds. In future work, we intend to model objects and backgrounds separately to obtain more refined generations.

6 Conclusion

We introduce Consist3D, a method to faithfully and photo-realistically personalize text-to-3D generation from a single view image, with background and object editable by text prompts, addressing the inconsistency issues in semantic, geometry, and saturation. Specifically, we propose a 3-stage framework with a semantic encoding, a geometric encoding stages and a low-scale score distillation sampling stage. The semantic token learned in the first encoding stage encourages Consist3D to be robust to shape estimation, the geometric token learned in the second stage encourages the generation to be consistent across different views, and both of the tokens are used in the third stage to encourage natural saturation of the 3D generation. Our method outperforms baselines quantitatively and qualitatively. Experiments on a wide range of images (including in-the-wild and synthesis images) demonstrate our approach can 1) generate high-fidelity 3D assets with consistency from one image. 2) change the background or Object of the 3D generations through editing the text prompts without changing the input image. Going forward, we plan to incorporate more geometric constraints into token training to further enhance 3D consistency.

References

- Cai, S.; Chan, E. R.; Peng, S.; Shahbazi, M.; Obukhov, A.; Van Gool, L.; and Wetzstein, G. 2023. Diff-Dreamer: Towards Consistent Unsupervised Single-view Scene Extrapolation with Conditional Diffusion Models. ArXiv:2211.12131 [cs].
- Cao, S.; Chai, W.; Hao, S.; and Wang, G. 2023. Image Reference-Guided Fashion Design With Structure-Aware Transfer by Diffusion Models. In *Proceedings of the IEEE/CVF Conference on Computer Vision and Pattern Recognition*, 3524–3528.
- Chai, W.; and Wang, G. 2022. Deep vision multimodal learning: Methodology, benchmark, and trend. *Applied Sciences*, 12(13): 6588.
- Chen, R.; Chen, Y.; Jiao, N.; and Jia, K. 2023. Fantasia3D: Disentangling Geometry and Appearance for High-quality Text-to-3D Content Creation. ArXiv:2303.13873 [cs].
- Deng, C.; Jiang, C. ; Qi, C. R.; Yan, X.; Zhou, Y.; Guibas, L.; and Anguelov, D. 2023. NeRDi: Single-View NeRF Synthesis With Language-Guided Diffusion As General Image Priors. 20637–20647.
- Dhariwal, P.; and Nichol, A. 2021. Diffusion Models Beat GANs on Image Synthesis. Technical Report arXiv:2105.05233, arXiv. ArXiv:2105.05233 [cs, stat] type: article.
- Gal, R.; Alaluf, Y.; Atzmon, Y.; Patashnik, O.; Bermano, A. H.; Chechik, G.; and Cohen-Or, D. 2022. An Image is Worth One Word: Personalizing Text-to-Image Generation using Textual Inversion. ArXiv:2208.01618 [cs].
- Gu, J.; Gao, Q.; Zhai, S.; Chen, B.; Liu, L.; and Susskind, J. 2023a. Learning Controllable 3D Diffusion Models from Single-view Images. ArXiv:2304.06700 [cs].
- Gu, J.; Trevithick, A.; Lin, K.-E.; Susskind, J.; Theobalt, C.; Liu, L.; and Ramamoorthi, R. 2023b. NerfDiff: Single-image View Synthesis with NeRF-guided Distillation from 3D-aware Diffusion. ArXiv:2302.10109 [cs].
- Hessel, J.; Holtzman, A.; Forbes, M.; Bras, R. L.; and Choi, Y. 2022. CLIPScore: A Reference-free Evaluation Metric for Image Captioning. ArXiv:2104.08718 [cs].
- Ho, J.; and Salimans, T. 2022. Classifier-Free Diffusion Guidance. ArXiv:2207.12598 [cs].
- Hu, E. J.; Shen, Y.; Wallis, P.; Allen-Zhu, Z.; Li, Y.; Wang, S.; Wang, L.; and Chen, W. 2021. LoRA: Low-Rank Adaptation of Large Language Models. ArXiv:2106.09685 [cs].
- Huang, L.; Chen, D.; Liu, Y.; Shen, Y.; Zhao, D.; and Zhou, J. 2023a. Composer: Creative and controllable image synthesis with composable conditions. *arXiv preprint arXiv:2302.09778*.
- Huang, Z.; Chan, K. C.; Jiang, Y.; and Liu, Z. 2023b. Collaborative diffusion for multi-modal face generation and editing. In *Proceedings of the IEEE/CVF Conference on Computer Vision and Pattern Recognition*, 6080–6090.
- Huang, Z.; Wu, T.; Jiang, Y.; Chan, K. C.; and Liu, Z. 2023c. ReVersion: Diffusion-Based Relation Inversion from Images. *arXiv preprint arXiv:2303.13495*.
- Jun, H.; and Nichol, A. 2023. Shap-E: Generating Conditional 3D Implicit Functions. ArXiv:2305.02463 [cs].
- Kawar, B.; Zada, S.; Lang, O.; Tov, O.; Chang, H.; Dekel, T.; Mosseri, I.; and Irani, M. 2023. Imagic: Text-based real image editing with diffusion models. In *Proceedings of the IEEE/CVF Conference on Computer Vision and Pattern Recognition*, 6007–6017.
- Lin, C.-H.; Gao, J.; Tang, L.; Takikawa, T.; Zeng, X.; Huang, X.; Kreis, K.; Fidler, S.; Liu, M.-Y.; and Lin, T.-Y. 2023. Magic3D: High-Resolution Text-to-3D Content Creation. ArXiv:2211.10440 [cs].
- Lin, K.-E.; Yen-Chen, L.; Lai, W.-S.; Lin, T.-Y.; Shih, Y.-C.; and Ramamoorthi, R. 2022. Vision Transformer for NeRF-Based View Synthesis from a Single Input Image. ArXiv:2207.05736 [cs].
- Liu, R.; Wu, R.; Van Hoorick, B.; Tokmakov, P.; Zakharov, S.; and Vondrick, C. 2023. Zero-1-to-3: Zero-shot One Image to 3D Object. ArXiv:2303.11328 [cs].
- Metzger, G.; Richardson, E.; Patashnik, O.; Giryes, R.; and Cohen-Or, D. 2022. Latent-NeRF for Shape-Guided Generation of 3D Shapes and Textures. ArXiv:2211.07600 [cs].
- Mou, C.; Wang, X.; Xie, L.; Zhang, J.; Qi, Z.; Shan, Y.; and Qie, X. 2023. T2i-adapter: Learning adapters to dig out more controllable ability for text-to-image diffusion models. *arXiv preprint arXiv:2302.08453*.
- Nichol, A.; Jun, H.; Dhariwal, P.; Mishkin, P.; and Chen, M. 2022. Point-E: A System for Generating 3D Point Clouds from Complex Prompts. ArXiv:2212.08751 [cs].
- Podell, D.; English, Z.; Lacey, K.; Blattmann, A.; Dockhorn, T.; Mller, J.; Penna, J.; and Rombach, R. 2023. SDXL: Improving Latent Diffusion Models for High-Resolution Image Synthesis. ArXiv:2307.01952 [cs].
- Poole, B.; Jain, A.; Barron, J. T.; and Mildenhall, B. 2022. DreamFusion: Text-to-3D using 2D Diffusion. ArXiv:2209.14988 [cs, stat].
- Radford, A.; Kim, J. W.; Hallacy, C.; Ramesh, A.; Goh, G.; Agarwal, S.; Sastry, G.; Askell, A.; Mishkin, P.; Clark, J.; Krueger, G.; and Sutskever, I. 2021. Learning Transferable Visual Models From Natural Language Supervision. ArXiv:2103.00020 [cs].
- Raj, A.; Kaza, S.; Poole, B.; Niemeyer, M.; Ruiz, N.; Mildenhall, B.; Zada, S.; Aberman, K.; Rubinstein, M.; Barron, J.; Li, Y.; and Jampani, V. 2023. DreamBooth3D: Subject-Driven Text-to-3D Generation. ArXiv:2303.13508 [cs].
- Ramesh, A.; Dhariwal, P.; Nichol, A.; Chu, C.; and Chen, M. 2022. Hierarchical Text-Conditional Image Generation with CLIP Latents. ArXiv:2204.06125 [cs] version: 1.
- Rombach, R.; Blattmann, A.; Lorenz, D.; Esser, P.; and Ommer, B. 2022. High-Resolution Image Synthesis with Latent Diffusion Models. ArXiv:2112.10752 [cs].
- Ruiz, N.; Li, Y.; Jampani, V.; Pritch, Y.; Rubinstein, M.; and Aberman, K. 2022. DreamBooth: Fine Tuning Text-to-Image Diffusion Models for Subject-Driven Generation. ArXiv:2208.12242 [cs].

- Saharia, C.; Chan, W.; Saxena, S.; Li, L.; Whang, J.; Denton, E.; Ghasemipour, S. K. S.; Ayan, B. K.; Mahdavi, S. S.; Lopes, R. G.; Salimans, T.; Ho, J.; Fleet, D. J.; and Norouzi, M. 2022. Photorealistic Text-to-Image Diffusion Models with Deep Language Understanding. ArXiv:2205.11487 [cs].
- Sanghi, A.; Jayaraman, P. K.; Rampini, A.; Lambourne, J.; Shayani, H.; Atherton, E.; and Taghanaki, S. A. 2023. Sketch-A-Shape: Zero-Shot Sketch-to-3D Shape Generation. ArXiv:2307.03869 [cs].
- Seo, J.; Jang, W.; Kwak, M.-S.; Ko, J.; Kim, H.; Kim, J.; Kim, J.-H.; Lee, J.; and Kim, S. 2023. Let 2D Diffusion Model Know 3D-Consistency for Robust Text-to-3D Generation. ArXiv:2303.07937 [cs].
- Tang, J.; Wang, T.; Zhang, B.; Zhang, T.; Yi, R.; Ma, L.; and Chen, D. 2023. Make-It-3D: High-Fidelity 3D Creation from A Single Image with Diffusion Prior. ArXiv:2303.14184 [cs].
- Tsalicoglou, C.; Manhardt, F.; Tonioni, A.; Niemeyer, M.; and Tombari, F. 2023. TextMesh: Generation of Realistic 3D Meshes From Text Prompts. ArXiv:2304.12439 [cs].
- Voynov, A.; Chu, Q.; Cohen-Or, D.; and Aberman, K. 2023. *P+*: Extended Textual Conditioning in Text-to-Image Generation. *arXiv preprint arXiv:2303.09522*.
- Wang, H.; Du, X.; Li, J.; Yeh, R. A.; and Shakhnarovich, G. 2022. Score Jacobian Chaining: Lifting Pretrained 2D Diffusion Models for 3D Generation. ArXiv:2212.00774 [cs].
- Wang, Z.; Lu, C.; Wang, Y.; Bao, F.; Li, C.; Su, H.; and Zhu, J. 2023. ProlificDreamer: High-Fidelity and Diverse Text-to-3D Generation with Variational Score Distillation. ArXiv:2305.16213 [cs].
- Wu, J. Z.; Ge, Y.; Wang, X.; Lei, W.; Gu, Y.; Shi, Y.; Hsu, W.; Shan, Y.; Qie, X.; and Shou, M. Z. 2023. Tune-A-Video: One-Shot Tuning of Image Diffusion Models for Text-to-Video Generation. ArXiv:2212.11565 [cs].
- Xing, Z.; Li, H.; Wu, Z.; and Jiang, Y.-G. 2022. Semi-Supervised Single-View 3D Reconstruction via Prototype Shape Priors. ArXiv:2209.15383 [cs].
- Xu, J.; Wang, X.; Cheng, W.; Cao, Y.-P.; Shan, Y.; Qie, X.; and Gao, S. 2023. Dream3D: Zero-Shot Text-to-3D Synthesis Using 3D Shape Prior and Text-to-Image Diffusion Models. 20908–20918.
- Xue, Z.; Song, G.; Guo, Q.; Liu, B.; Zong, Z.; Liu, Y.; and Luo, P. 2023. RAPHAEL: Text-to-Image Generation via Large Mixture of Diffusion Paths. ArXiv:2305.18295 [cs].
- Yang, J.; Wang, H.; Xiao, R.; Wu, S.; Chen, G.; and Zhao, J. 2023. Controllable Textual Inversion for Personalized Text-to-Image Generation. *arXiv preprint arXiv:2304.05265*.
- Yu, C.; Zhou, Q.; Li, J.; Zhang, Z.; Wang, Z.; and Wang, F. 2023. Points-to-3D: Bridging the Gap between Sparse Points and Shape-Controllable Text-to-3D Generation. ArXiv:2307.13908 [cs].
- Zhang, L.; and Agrawala, M. 2023. Adding Conditional Control to Text-to-Image Diffusion Models. ArXiv:2302.05543 [cs].
- Zhang, Y.; Huang, N.; Tang, F.; Huang, H.; Ma, C.; Dong, W.; and Xu, C. 2023. Inversion-based style transfer with diffusion models. In *Proceedings of the IEEE/CVF Conference on Computer Vision and Pattern Recognition*, 10146–10156.